



HAL
open science

Anticancer properties of lipid and poly(ϵ -caprolactone) nanocapsules loaded with ferrocenyl-tamoxifen derivatives

Feten Najlaoui, Pascal Pigeon, Sonia Aroui, Mylène Pezet, Lucie Sancey, Naziha Marrakchi, Ali Rhouma, Gérard Jaouen, Michel de Waard, Benoît Busser, et al.

► To cite this version:

Feten Najlaoui, Pascal Pigeon, Sonia Aroui, Mylène Pezet, Lucie Sancey, et al.. Anticancer properties of lipid and poly(ϵ -caprolactone) nanocapsules loaded with ferrocenyl-tamoxifen derivatives. *Journal of Pharmacy and Pharmacology*, 2018, 70 (11), pp.1474-1484. 10.1111/jphp.12998 . hal-01861749

HAL Id: hal-01861749

<https://hal.science/hal-01861749v1>

Submitted on 5 Nov 2018

HAL is a multi-disciplinary open access archive for the deposit and dissemination of scientific research documents, whether they are published or not. The documents may come from teaching and research institutions in France or abroad, or from public or private research centers.

L'archive ouverte pluridisciplinaire **HAL**, est destinée au dépôt et à la diffusion de documents scientifiques de niveau recherche, publiés ou non, émanant des établissements d'enseignement et de recherche français ou étrangers, des laboratoires publics ou privés.

1 **Anticancer properties of lipid and poly(ϵ -caprolactone) nanocapsules loaded with**
2 **ferrocenyl tamoxifen derivatives**

3 Feten Najlaoui^{1,2}, Pascal Pigeon (PhD)^{3,4}, Sonia Aroui (PhD)⁵, Mylène Pezet⁶ (PhD), Lucie Sancey
4 (PhD)⁶, NazihaMarrakchi (Professor)¹, Ali Rhouma (Professor)⁷, Gérard Jaouen (Professor)^{3,4}, Michel
5 De Waard (PhD)⁸, Benoit Busser (PharmD, PhD)⁶, Stéphane Gibaud (PharmD, PhD)²
6

7 ¹Laboratoire des Venins et Biomolécules Thérapeutiques LR11IPT08, Institut Pasteur de Tunis, 13, Place
8 Pasteur, 1002 Tunis, Tunisia.

9 ²Université de Lorraine, EA 3452/CITHEFOR, 5 rue Albert Lebrun (Faculté de Pharmacie), F-54000 Nancy,
10 France.

11 ³Chimie ParisTech, 11 rue Pierre et Marie Curie, Paris F75231 Paris Cedex 05, France.

12 ⁴Sorbonne Universités, UPMC Université Paris 6, Institut Parisien de Chimie Moléculaire (IPCM) – UMR 8232,
13 4 place Jussieu, 75252 Paris Cedex 05, France.

14 ⁵Laboratory of Biochemistry, Molecular Mechanisms and Diseases Research Unit, UR12ES08, Faculty of
15 Medicine, University of Monastir.

16 ⁶University Grenoble Alpes, IAB Inserm U1209 / CNRS UMR 5309, Grenoble University Hospital, F-38000
17 Grenoble, France.

18 ⁷Research Unit of Plant Protection and Environment, Olive Tree Institute, Mahrajene City BP 208, 1082 Tunis,
19 Tunisia

20 ⁸Institut du Thorax, INSERM UMR 1087 / CNRS UMR 6291, 8 quai Moncousu, Nantes University, Labex Ion
21 Channels, Science & Therapeutics, 44007 Nantes Cedex 1, France.

22

23 **Author to whom correspondence should be sent:**

24 Stéphane Gibaud - Université de Lorraine, EA 3452/CITHEFOR - 5, rue Albert Lebrun
25 (Faculté de Pharmacie) - F-54000 Nancy, France; Tel : +33 3 72 74 73 06; Mobile : +33 6 68
26 47 4 00; email: stephane.gibaud@univ-lorraine.fr

27

28 **Abstract**

29 **Objective:** We synthesized new tamoxifen derivatives as anticancer drug candidates and
30 elaborated on convection-enhanced delivery (CED) as strategy for delivery.

31 **Methods:** To overcome the issue of their poor solubility, these ferrocenyl-tamoxifen
32 derivatives were esterified and encapsulated into different nanocarriers, i.e lipid (LNC) and
33 polymeric nanocapsules (PNL-NC). We describe the chemistry, the encapsulation and the
34 physicochemical characterization of these formulations.

35 **Key findings:** Starting compounds [phthalimido-ferrocidiphenol and succinimido-
36 ferrocidiphenol], esterified prodrugs and their nanocapsules formulations were characterized.
37 These drug candidates displayed a strong *in vitro* activity against breast and glioblastoma
38 cancer cells. The ester prodrugs were toxic for glioblastoma cells ($IC_{50} = 9.2 \times 10^{-2} \mu M$ and
39 $6.7 \times 10^{-2} \mu M$ respectively). The IC_{50} values for breast cancer cells were higher for these
40 compounds.

41 The encapsulation of the esterified compounds in LNCs (≈ 50 nm) or PCL-NCs (≈ 300 nm)
42 did not prevent their efficacy on glioblastoma cells. These anticancer effects were due to both
43 a blockade in the S-phase of the cell cycle and apoptosis. Moreover, the tamoxifen
44 derivatives-loaded nanocapsules induced no toxicity for healthy astrocytes and showed no
45 hemolytic properties. Loaded Lipid Nanocapsules (LNC) presented interesting profiles for the
46 optimal delivery of active compounds.

47 **Conclusion:** Phthalimido- and Succinimido-esters represent an innovative approach to treat
48 cancers with cerebral localizations such as glioblastoma or brain metastases from breast
49 cancers.

50

51 **Keywords (5):** Lipid nanocapsules, polymer nanocapsules, ferrocenyl tamoxifen
52 derivatives, breast cancer, glioblastoma.

53 1. Introduction

54 Tamoxifen has been used for endocrine therapy to treat breast cancer for many years. This
55 selective estrogen receptor modulator (SERM) possesses an active metabolite named
56 hydroxytamoxifen that competitively binds to estrogen receptor (ER) and thus inhibits cancer
57 cell proliferation.^[1] Nonetheless, tamoxifen efficacy is only observed against estrogen
58 receptor-positive tumors (ER⁺), but resistance occurs after long-term usage.^[2] Importantly,
59 tamoxifen is also able to treat other cancers, such as glioblastoma, in association with the
60 standard of care, which is temozolomide.^[3] The embedding of a ferrocenyl unit into the
61 tamoxifen skeleton can lead to a new family of breast cancer drug candidates named
62 hydroxyferrocifens.^[4,5] Hydroxyferrocifens have the advantage of dual functionality.
63 Effectively, these molecules have endocrine-modulating properties along with cytotoxic
64 activities. A variety of hydroxyferrocifens were synthesized by structure-reactivity
65 relationship studies.^[6] The activity remains when the dimethylaminoalkyl chain, which is
66 inherited from the hydroxytamoxifen, is suppressed, leading to the ferrocidiphenol series.
67 Among this series, some compounds with modification at the ethyl group, that is also
68 inherited from hydroxytamoxifen, had better activity, in particular when a polar group was
69 fixed at the end of the alkyl chain.^[7,8] Thus, the introduction of a polar imide group gave rise
70 to ferrocidiphenol (Ferr) compounds, namely phthalimido-ferrocidiphenol (PhtFerr)
71 (C₃₅H₂₉FeNO₄) and succinimido-ferrocidiphenol (SuccFerr) (C₃₁H₂₉FeNO₄), that were found
72 to be very effective on breast cancer cells (MDA-MB-231) and, more surprisingly, on human
73 glioblastoma cancer cells (U87).^[9] The mechanism underlying the Ferr cytotoxicity is only
74 partly understood. Previous *in vitro* studies demonstrated that at least some Ferr metabolites
75 produced in the cell are electrophilic quinonemethides that can induce growth arrest with

76 senescence and apoptosis phenomena.^[10,11] Recently, adducts of these quinonemethides with
77 compounds bearing thiol functional group, as models of some cellular nucleophiles were
78 identified.^[12]

79 Metal-based anticancer drugs, such as PhtFerr and SuccFerr, are very hydrophobic
80 compounds that cannot be formulated in aqueous solutions easily.^[13] Therefore, we both
81 synthesized their respective ester prodrugs Phtester and Succester and also encapsulated them
82 into nanocarriers to overcome the issue of their poor solubility. We compared two different
83 formulations, *ie* lipid nanocapsules (LNCs) and poly(ϵ -caprolactone) nanocapsules (PCL-
84 NCs), for encapsulation efficiency and release of the prodrugs of interest. These nanocapsules
85 can be considered as platforms for a future development but, in a first step, they could be
86 administered locally by Convection-Enhanced Delivery (CED).

87 LNCs (~100 nm) have a special structure between those of polymer nanocapsules and
88 liposomes. These particles have various advantages, including a solvent-free manufacturing
89 process and a prolonged physical stability of more than 18 months.^[14] Moreover, they allow
90 the transport of multiple types of drugs, including lipophilic anticancer drugs such as
91 paclitaxel, docetaxel, doxorubicin, hydroxytamoxifen, and etoposide;^[15] DNA and small
92 interfering RNAs;^[16,17] radionuclides;^[18,19] and nuclease-resistant locked nucleic acids,^[20]
93 offering a pharmaceutical solution for their parenteral administration.

94

95 PCL-NCs are larger vesicular systems (~300 nm) in which a lipophilic drug can be dissolved
96 in an oily core and surrounded by a polymeric shell, allowing the drug to be absorbed onto the
97 surface or entrapped within the nanocarriers.^[21] Some of the advantages of polymeric
98 nanocapsules are their high loading capacity for lipophilic drugs, the protection they provide

99 against enzymatic degradation and their physicochemical stability. Moreover, PCL is a
100 polyester polymer that is biodegradable and biocompatible.^[22] PCL is also considered a well-
101 tolerated nanocarrier with very slow degradation.^[23] It was recently used as a safe scaffold for
102 brain delivery of therapeutic agents.^[24] This paper details the physicochemical
103 characterization of PhtFerr and SuccFerr and the synthesis of their respective esterified-
104 derivatives Phtester and Succester. All of these compounds were loaded into LNCs and PCL-
105 NCs. We studied the *in vitro* drug release profile of the encapsulated prodrugs and their
106 cytotoxicity against glioblastoma U87 cell lines and human breast MDA-MB-231 cancer (this
107 latter cell line is known to be very sensitive to ferrocenylphenols). All these novel tamoxifen
108 derivatives were more toxic for cancer cells compared to the parent drug tamoxifen, but less
109 toxic for normal astrocytes. The strong and promising anticancer effect was demonstrated by
110 both an efficient blockade of the cell cycle and also proapoptotic activity in breast and
111 glioblastoma cancer cells.

112

113 **2. Material and Methods**

114 **2.1. Chemistry**

115 Reagents, molecules and chemical reactions are described in the supplementary material S1.

116 The synthesis of PhtFerr and compound X have been previously described.^[9]

117 The complete chemical synthesis is detailed in S1. Measurements of the octanol/water
118 partition coefficient (log Po/w) were made using high-performance liquid chromatography
119 (HPLC) according to a method described previously.^[25]

120

121 **2.2. Solubility studies**

122 Unless otherwise specified, all of the solvents were obtained from either Gattefossé (Nanterre,
123 France) or Sigma Aldrich (Saint Quentin Fallavier, France).

124 The solubility of Phtester and Succester was determined as follows: two milliliters of each
125 vehicle was added to screw-cap vials containing an excess of each of the Phtester and
126 Succester compounds (*ie* 500 mg). The mixture was heated in a shaking water bath
127 (Memmert, Schwabach, Deutschland; 25°C, 48 h, 60 strokes/min) to improve the dissolution.
128 When equilibrium was achieved, the mixture was centrifuged at 1400 × g for 5 min, and the
129 undissolved powder was discarded. Concentrations were determined by HPLC.

130

131 **2.3. Preparation and loading of lipidic nanocapsules (LNC)**

132 Phtester-LNCs and Succester-LNCs were prepared by a one-step process based on a phase-
133 inversion temperature method described elsewhere.^[26] To obtain LNCs, Solutol® HS15 (17%
134 w/w), Lipoid® S75 (1.5% w/w, Lipoid Kosmetic, Grasse, France), Labrafac® (18.3% w/w),

135 Phtester or Succester (1.7%), NaCl (1.75% w/w) and water (59.75% w/w) were mixed and
136 heated under magnetic stirring up to 85°C. Three cycles of progressive heating and cooling
137 between 85°C and 60°C were then carried out and followed by an irreversible shock induced
138 by dilution with 2°C deionized water (45 or 70% v/v) added to the mixture when it had
139 reached 70–75°C. The resulting suspension was passed through a 0.2 µM filter to remove the
140 free drug. The drug candidate load was expressed as the weight of drug in the lipid phase (in
141 mg/g; after freeze-drying). The encapsulation yield (in %) was the amount of drug obtained at
142 the end of the process divided by the initial amount of drug.

143

144 **2.4. Preparation and loading of polymeric nanocapsules (PCL-NCs)**

145 Phtester PCL-NCs and Succester PCL-NCs were prepared by a nanoprecipitation method that
146 consisted of dissolving the molecules of interest (*ie* Phtester or Succester) in an organic phase:
147 1% triethyl citrate (with 5 mg/mL of PhtFerr or Succester), 10% alcoholic solution of lecithin
148 (5 mg of lecithin/mL, Sigma Aldrich, Saint Quentin Fallavier, France) and 89% solution of
149 PCL in acetone (1% of PCL, Sigma Aldrich, Saint Quentin Fallavier, France). This organic
150 phase (10 mL) was added drop-wise under magnetic stirring to an aqueous solution of 10%
151 Pluronic F68 (20 mL). Acetone and a portion of the water were then removed by evaporation
152 in a vacuum at +40°C (Rotavapor Heidolf 94200) to reach a final volume of 15 mL. PCL-NCs
153 were then purified on a gel column (ACA Ultrogel[®] 54, Sigma Aldrich, Saint Quentin
154 Fallavier, France). The drug candidate load was expressed as the weight of drug after freeze-
155 drying (in mg/g of dried nanocapsules). The encapsulation yield (in %) was the amount of
156 drug obtained after purification divided by the initial amount of drug.

157

158

159 **2.5. Freeze-drying of nanocapsules**

160 The samples were frozen in liquid nitrogen and freeze-dried (Labconco Freezone 6L). The
161 temperature of each sample was equilibrated at -20 °C for 72 h. After lyophilisation, the
162 samples were stored at -20°C until further use.

163

164 **2.6. Nanoparticles size and *zeta* potential**

165 The size and *zeta* potential distribution of the nanocarriers were analyzed using a Malvern
166 Zetasizer® Nano Series DTS 1060 (Malvern Instruments S.A., Worcestershire, UK) operating
167 at an angle of 90° and a temperature of 25°C (n=3). The nanocarriers were diluted 1:100 (v/v)
168 in deionized water to ensure good scatter intensity on the detector. The *zeta* potential (n=3)
169 was measured at pH 7.1 at 25°C at the same dilution using the following specifications:
170 medium viscosity = 0.91 cP; refractive index (RI) = 1.33.

171

172 **2.7. Drug payload in nanocarriers and encapsulation efficiency**

173 Nanocarriers were first dissolved in acetonitrile. Then, the payload and encapsulation
174 efficiency of LNCs and PCL-NCs were measured using an HPLC protocol. Twenty
175 microliters of sample was injected into a C₁₈ column (Nucleosil®, 5 µm, 0.46 mm, 25 cm;
176 Macherey Nagel, Eckbolsheim, France) using an autosampler (Spectra Physics AS1000). The
177 mobile phase was a mixture of acetonitrile and water (65:35, v/v) with a flow rate of 1.5
178 mL/min (Spectra Physics P1000XR; Thermo Electron S.A., Courtaboeuf, France). UV
179 spectrophotometry was used to detect absorbance at 254 nm (Spectra Physics UV1000), and
180 the peak area was used for quantification.

181

182 **2.8. *In vitro* drug release from nanocarriers**

183 The dialysis method was used as follows. Five milligrams of the lyophilized Phtester PCL-
184 NCs, Succester PCL-NCs, Phtester LNCs, Succester LNCs, or Succester powder or
185 Phtester powder were poured into 2 ml of 1% Tween[®] 20 and then transferred to a dialysis
186 bag (molecular weight cutoff 14 kDa, Spectra/Por, Spectrum Laboratories, Paris, France).
187 Each bag was placed into a bath of 498 mL of 1% Tween[®] 20 (pH 6.8). These preparations
188 were placed in a bath shaking at 200 strokes/min at 25°C (Heito, France). One milliliter
189 aliquots were taken at various intervals during the release period (24 h) and analyzed by
190 HPLC to assess their drug content. The results are presented as the mean \pm standard
191 deviation (SD) of 3 experiments.

192

193 **2.9. *In vitro* cytotoxicity**

194 The cytotoxic activity of Phtester LNCs, Phtester PCL-NCs, Succester LNCs, Succester
195 PCL-NCs, Phtester, Succester, PhtFerr and SuccFerr was assessed using healthy astrocytes,
196 the U87 human glioblastoma cell line and the human breast cancer (MDA-MB-231) cell
197 line. Purified newborn rat primary astrocytes were obtained by mechanical dissociation
198 from cultures of cerebral cortex (authorization n° 2015.080410145453v3) as previously
199 described.^[27] Fisher male rats were obtained from Charles River Laboratories France
200 (L'Arbresle, France).

201 The U87 and MDA-MB-231 cell lines were obtained from ATCC (Molsheim, France).

202 The cells were grown at 37 °C/5% CO₂ in Dulbecco's modified Eagle medium (DMEM)
203 (Invitrogen[™], Life Technologies, Carlsbad, MA, USA) with glucose and L-glutamine
204 (Cergy-Pontoise, France), 10% fetal calf serum (FCS) (BioWhittaker) and 1% antibiotic
205 and antimycotic solution (Sigma, Saint-Quentin Fallavier, France). Phtester and Succester
206 were dissolved in 1% dimethylsulfoxide (DMSO), whereas Phtester PCL-NCs, Phtester

207 LNCs, Succester LNCs, Succester PCL-NCs, blank LNCs and blank PCL-NCs were
208 dispersed directly in DMEM. Tamoxifen was tested as a control drug.

209 All of the cells were seeded in sterile 96-well plates for 12 h with 100 μ L of medium
210 (5×10^3 /well). Cells were then exposed to varying amounts of the indicated drug candidates
211 at concentrations ranging from 10^{-3} to 10^{-9} M for 96 h at 37 °C. Blank nanocarriers were
212 tested at an equivalent excipient concentration (compared to Phtester- or Succester-loaded
213 PCL-NCs or LNCs). Cell cytotoxicity was then measured by a colorimetric assay using 3-
214 (4,5-dimethylthiazol-2-yl)-2,5-diphenyltetrazolium bromide (MTT). Ninety microliters of
215 DMEM medium with 10% MTT was added to each well and incubated for 2-4 h at 37 °C.
216 MTT was removed, followed by addition of solubilizing solution (100 μ L DMSO),
217 resulting in crystalline formazan formation. The absorbance was measured at 560 nm using
218 a Beckman Coulter™ AD340S spectrophotometer. The absorbance is proportional to the
219 number of viable cells, and survival was calculated as a percentage of the values measured
220 for untreated cells.

221

222 **2.10. Cell cycle analysis**

223 In 6-well culture plates, 5×10^5 U87 cells were seeded in 6-well culture plates with 2 mL of
224 medium per well. After 12 h, the culture medium was removed, and cells were treated with
225 10 μ M of Phtester PCL-NCs, Phtester LNCs, Succester PCL-NCs, Succester LNCs, Phtester,
226 Succester, PhtFerr, SuccFerr or blank formulations (PCL-NCs and LNCs); the culture plates
227 were incubated for 96 h at 37 °C. At the end of the experiment, cells were trypsinized, washed
228 twice with PBS (without Ca^{2+} and Mg^{2+}) and incubated with cold ethanol overnight at 4 °C.
229 Cells were then centrifuged, washed once with PBS and then incubated with 0.5 mL PI/RNase
230 (30 min, in the dark). The cell cycle was analyzed with an Accuri C6 flow cytometer (BD

231 Biosciences) in at least three independent experiments, with 50,000 cells being measured in
232 each sample, and data were analyzed by FCS Express 5 Software (De Novo Software, USA).

233

234 **2.11. Cell apoptosis assay**

235 The U87 cell line was incubated with 10 μ M of different compounds (Phtester PCL-NCs,
236 Phtester LNCs, Succester-PCL-NCs, Succester LNCs, Phtester, Succester, PhtFerr, or
237 SuccFerr) for 96 h. Apoptotic cell death was revealed by flow cytometry using a
238 phycoerythrin-conjugated monoclonal active caspase-3 antibody kit (BD Pharmingen, Le
239 Pont de Claix, France) following the manufacturer's instructions. The cells were analyzed
240 with a BD-Accuri C6 flow cytometer, and the data were analyzed by FCS Express 5
241 Software. The percentage of apoptosis was obtained comparing it with the positive control

242

243 **2.12. Statistical analysis**

244 Statistical analyses were performed using GraphPad Prism 6 software (GraphPad Prism, La
245 Jolla, USA). Kruskal–Wallis test (nonparametric) was used for cell cultures. Dunn's post-test
246 (nonparametric) was then used for multiple comparisons. Mann and Whitney test was used to
247 compare the release of the complexes for each formulation.

248

249 **3. Results**

250

251 **3.1. Chemistry**

252 PhtFerr and SuccFerr were synthesized by substitution of the chlorine atom of 5-chloro-2-
253 ferrocenyl-1,1-bis-(4-hydroxyphenyl)-pent-1-ene (compound X) with an imide (succinimide,
254 Figure 1 and S1). The ester prodrugs (N-{4-ferrocenyl-5,5-bis-(4-acetoxyphenyl)-pent-4-
255 enyl}phthalimide Phtester) and (N-{4-ferrocenyl-5,5-bis-(4-acetoxyphenyl)-pent-4-
256 enyl}succinimide Succester) were obtained by acetylation of PhtFerr and SuccFerr,
257 respectively (Figure 1). The characterization of the products is in supplementary materials S1.

258

259 **3.2. Solubility studies**

260 To find the optimal formulation of LNCs and PCL-NCs, we tested the dissolution properties
261 of various surfactants [Solutol[®] HS 15 (polyoxyethylated 12-hydroxystearic acid),
262 triethylcitrate, Capryol[®] 90 (propylene glycol monocaprylate), Transcutol[®] HP (highly
263 purified diethylene glycol monoethyl ether), Labrasol[®] ALF (caprylocaproyl polyoxyl-8
264 glycerides), Maisine[®] 35-1 (glycerol monolinoleate), Miglyol[®] 812 (caprylic/capric
265 triglyceride, Dynamit Nobel, Leverkusen, Germany), Labrafac[®] (medium-chain triglycerides),
266 Tween[®] 20 (polysorbate 20), Tween[®] 80 (polysorbate 80)] and oils [olive oil, benzylbenzoate,
267 ethyl oleate, Captex[®] 355 (glyceryltricaprylate/tricaprate), Triacetin (1,2,3-
268 triacetoxyp propane)].

269

270 The results of solubility studies are reported in Table 1. Among the surfactants, Solutol[®]
271 HS15 and Lafrac[®], usually used to make LNCs, have very good solubilization capacities.

272 Triethylcitrate, which has previously been used to make PCL-NCs, has quite similar
273 properties. Finally, Tween[®] 20 was used for solubility experiments.

274 In each formulation (*ie*, LNCs or PCL-NCs), the ferrocenyl-tamoxifen derivatives were
275 dissolved in oily droplets. Surfactants were used to increase the solubility of both Phtester and
276 Succester.

277

278 **3.3. Preparation and characterization of Phtester- and Succester-loaded nanocarriers**

279 Because Labrafac[®] and Solutol[®] HS15 were included in the formulation of LNCs,^[26] the
280 dissolutions of the drug candidates were very easy.

281 By mixing Phtester or Succester with excipients (*ie*, Labrafac[®], Solutol[®] HS15 or Lipoid[®]) at
282 well-characterized concentrations described by a ternary diagram^[26] and by applying the
283 phase-inversion process, Phtester LNCs and Succester LNCs were obtained. Their size ranges
284 were very narrow with diameters between 53.4 ± 0.9 nm and 57.8 ± 2.0 nm (before
285 lyophilisation), respectively, depending on the anticancer drug candidates payload
286 (polydispersity index (PI) < 0.15) (Table 2). There was no significant difference before and
287 after lyophilisation. Phtester LNCs and Succester LNCs were also characterized in terms of
288 surface charge: *zeta* potential values were -10.8 ± 2.0 and -11.1 ± 1.3 mV, respectively.
289 These physicochemical properties (Table 2) were very similar to those of the previously
290 studied standard blank LNCs.^[28,29] Indeed, because of the presence of PEG dipoles in their
291 shells, 50-nm blank LNCs have a low *zeta* potential of approximately -10 mV.^[30] The
292 possible presence of the active drug on the surface did not affect the *zeta* potential values,
293 which suggests that Phtester and Succester were efficiently encapsulated in the LNCs. Like
294 many other hydrophobic drugs,^[31-33] both compounds were mostly encapsulated in the LNCs
295 with a high encapsulation yields above 92% (Table 2).

296 Phtester PCL-NCs and Succester PCL-NCs were obtained by nanoprecipitation. They had
297 sizes of 303 ± 12 nm and 295 ± 18 nm, respectively, that were similar to the size of the blank
298 ones (289 ± 7 nm). The PCL-NCs loaded with Phtester and Succester exhibited negative
299 charges of -18.2 ± 0.7 mV and -14.9 ± 2.4 mV, respectively. The incorporation of Phtester
300 and Succester in PCL-NCs was very effective, as demonstrated by the high encapsulation
301 yield and the *zeta* potential (Table 2).

302

303 **3.4. Pharmaceutical properties**

304 **3.4.1. *In vitro* release study**

305 Phtester and Succester release studies were performed by a dialysis method. Under our
306 conditions, the solubility of Phtester and Succester in the external compartment
307 (Tween[®] 20, 1%) was 0.036 mg and 0.041 mg, respectively. The loaded LNC and PCL-NC
308 formulations were both studied. Figure 2 illustrates the dissolution profiles obtained. Phtester
309 PCL-NCs and Succester PCL-NCs were the most efficient formulations for effective drug
310 release of greater than 70% after 12 h, whereas the diffusion from Phtester LNCs, Phtester,
311 Succester-LNCs and Succester were quite slow, reaching only 30-40% release of the loaded
312 drug candidates in the external phase after 24 h.

313

314

315

316 3.4.2. *In vitro* cytotoxicity on U87 cell lines

317 We performed MTT assays to evaluate the influence of the drug candidates on the viability of
318 healthy astrocytes, MDA-MB-231 cells and U87 cells after treatment with Phtester- and
319 Succester-loaded nanocapsules. A solution of 1% DMSO did not show any sign of toxicity.
320 Therefore, the negative control was composed of the DMSO solution used to dissolve Phtester
321 and Succester, and the corresponding viability was considered to be 100%. The blank
322 formulations (nanocarriers alone) were non-toxic to breast cancer and glioblastoma cells and
323 normal astrocytes in the micromolar range, as indicated in Table 3; the toxicity of tamoxifen
324 was quite similar on the tree cell lines.

325 PhtFerr and its prodrug Phtester were highly toxic to U87 cells, with very low IC_{50} values of
326 $1.6 \times 10^{-1} \mu\text{M}$ and $9.2 \times 10^{-2} \mu\text{M}$, respectively. The IC_{50} values for MDA-MB-231 cells were
327 slightly higher for these compound but differences were not significant (Table 3; Kruskal
328 Wallis, Dunn's post hoc test vs U87 : $p > 0.05$).

329 The IC_{50} of PhtFerr and its prodrug Phtester were significantly higher (i.e. less toxic) on
330 astrocytes (Table 3; Kruskal Wallis, Dunn's post hoc test vs U87: $p < 0.05$). When
331 encapsulated, the Phtester drug candidate conserved an important toxicity for glioblastoma
332 cells.

333 Similarly, SuccFerr and its prodrug Succester were highly toxic to U87 cells, with very low
334 IC_{50} values of $2.7 \cdot 10^{-2} \mu\text{M}$ and $6.7 \cdot 10^{-2} \mu\text{M}$, respectively (Table 3; Kruskal Wallis, Dunn's
335 post hoc test vs U87: $p < 0.05$). The encapsulation of Succester in LNCs or PCL-NCs did not
336 alter or prevent the efficacy of the drug candidates on glioblastoma cells.

337 Importantly, Phtester- and Succester-loaded formulations did not alter cell viability for
338 healthy astrocytes at the micromolar range.

339

340

341 **3.4.3. Cell cycle analysis**

342 The different treatments induced a major blockade in the subG1 and in S phases of the cell
343 cycle (Figure 3) compared to their respective controls. This is in agreement with the cytotoxic
344 activity of the different treatments (Table 3). Such an increase in the subG1 cell population
345 revealed an alteration of the DNA content within the treated cells, which could occur either by
346 necrosis or apoptosis.

347

348 **3.4.4. Cell apoptosis assay**

349 To investigate whether the native drugs candidates and their encapsulated forms induced
350 apoptosis in U87 glioblastoma cells, we measured the induction of apoptosis with an active
351 caspase-3 assay (Figure 4). All of the molecules and nanoformulations induced a significant
352 increase in apoptosis after 96 h of treatment at 10 μ M. We also observed a major pro-
353 apoptotic effect of the Phtester PCL-NC formulation. All together, these results confirmed
354 that the increased subG1 fractions observed (Figure 3) were due to the induction of apoptosis.

355

356

357 4. Discussion

358 Both PhtFerr and SuccFerr are tamoxifen derivatives and promising drug candidates for the
359 treatment of cancer. However, these compounds are almost insoluble in water, and it is
360 necessary to adapt their formulations to increase water solubility. Therefore, we decided to
361 modify their chemistry by means of esterification and to encapsulate the resulting prodrugs
362 Phtester and Succester into PCL-NCs and LNCs. Since we think that an intravenous
363 administration of these nanocapsules could induce hepatic toxicity, we proposed these
364 formulations for a Convection-Enhanced Delivery (CED) for further *in vivo* experiments.

365 Polyester nanocapsules (PCL-NCs) can be produced by a solvent evaporation method:
366 polymers and drug candidates are dissolved in an organic phase (*ie* oils and volatile water-
367 miscible solvents) constituting the inner phase of an oil-in-water emulsion (O/W). The
368 diffusion of the organic solvent into the aqueous phase causes precipitation of the polymer at
369 the interface, and the final nanocarriers are made of an oily core and a polymeric shell. The
370 blank PCL-NC formulation did not show any particular toxicity in our various cell models, as
371 indicated by the very high IC₅₀ values on normal and cancer cells (Table 3).

372

373 In the present study, loaded LNCs and PCL-NCs had different drug release kinetics. Loaded
374 PCL-NCs released approximately 60% of the initial drug amount within 6 h. This is
375 considered very substantial compared to the release properties of LNCs, which showed a
376 much slower release pattern (7 and 16%, respectively, for Phtester LNCs and Succester LNCs
377 within 6 h). Consequently, both nanocarriers and their associated release patterns could be
378 suitable for cancer treatment delivery, allowing fast or delayed delivery, respectively.

379 Considering drug-loaded nanocapsules, the mechanisms of cytotoxicity are a complex matter.
380 The commonest method for lipophilic drugs to pass through cell membranes is passive

381 diffusion but if the drug is included in nanocarriers, the diffusion can occur only after the
382 release in the medium (which is in favor of a lower toxicity); simultaneously, an adsorption of
383 the nanocarriers on the surface can induce a direct toxicity or be followed by an uptake of the
384 particles (phagocytosis, macropinocytosis, caveolae-mediated pathways, ...). Some of these
385 mechanisms have been reported for U87 (eg phagocytosis^[34]) and for MDA-MB-231 (eg
386 clathrin- and caveolae-mediated pathways^[35]). The accurate mechanisms of uptake have not
387 been explored in this study; nevertheless, the *in vitro* experiments conducted with the
388 nanocapsules loaded with hydroxyferrocifens ester prodrugs (*ie* Succester and Phtester)
389 showed more cytotoxicity in cancer cells (MDA-MB-231 and U87) than in healthy astrocytes.
390 This important result suggests that targeting either glioblastoma cells or brain metastases from
391 breast cancer with encapsulated esterified hydroxyferrocifens could prevent off-target toxicity
392 to normal surrounding healthy brain tissue.

393 The anticancer activity of these Ferr derivatives encapsulated into LNCs and PCL-NCs
394 resulted from a combination of cytostatic effects (S-phase blockade) and cytotoxic effects
395 (induction of apoptosis).

396 Importantly, LNCs have high drug-loading capacity, long-term physical stability, and a
397 sustained drug release pattern, and they are able to enter the intracellular compartment of
398 epithelial or glioma cells.^[36] For all of these reasons, it is widely accepted that LNCs
399 represent one of the most promising nanoplatforms for central nervous system delivery.^[36]

400

401 **5. Conclusion**

402

403 Taken together, our results indicate that the Phtester and Succester prodrugs are ferrocenyl-
404 tamoxifen derivatives that are active against breast cancer and glioblastoma cells.

405 Encapsulation of these molecules in LNCs does not modify their anticancer properties against
406 these cell lines, though it does increase their solubility without adding toxicity to healthy
407 astrocytes. We postulate that these formulations could be developed for CED administration
408 and should be further explored for cancers located in the CNS, such as brain metastases of
409 breast cancer or glioblastoma.

410

411

412

413

414

415 **Acknowledgements:** Feten Najlaoui thanks the University of Cartage for financial support
416 during the PhD thesis process. Michel De Waard acknowledges financial support from
417 Inserm.

418

419 **Conflict of interest:** The authors claim that no conflict of interest, financial or otherwise.

420

421
422
423
424

Table 1: Solubility of Phtester and Succester in various oils and surfactants

Vehicle	HLB*	Solubility of Phtester (mg/mL)	Solubility of Succester (mg/mL)
Tween® 20	16.7	408 ± 12	312 ± 15
Tween® 20 - 1%	16.7	1.2	6.2
Tween® 20 - 5%	16.7	15	19
Tween® 20 - 10%	16.7	26	15
Tween® 20 - 20%	16.7	43	29
Tween® 80	15	532 ± 8	619 ± 56
Solutol® HS 15	14-16	309 ± 61	408 ± 12
Labrasol® ALF	12	10.0 ± 0.1	11 ± 1
Triethylcitrate	8.1	660 ± 17	432 ± 38
Capryol® 90	6	3.8 ± 0.1	1.4 ± 0.1
Transcutol® HP	4.2	39 ± 0.1	20 ± 3
Maisine® 35-1	4	6.0x10 ⁻² ± 0.1x10 ⁻²	1.2 ± 0.1
Miglyol® 812	15.4	7.2x10 ⁻⁴ ± 0.8x10 ⁻⁴	6.1x10 ⁻⁴ ± 0.1x10 ⁻⁴
Labrafac®	6	460 ± 5	465 ± 12
Benzoate benzyle	1	0.32 ± 0.01	2.0 ± 0.6
Triacetin®	Oil	5.7 ± 0.4	8.2 ± 0.2
Ethyl oleate	Oil	9.1x10 ⁻⁴ ± 0.6x10 ⁻⁴	11.10 ⁻⁴ ± 1.10 ⁻⁴
Captex® 355	Oil	9.3 ± 0.1	8.5 ± 0.1
Olive oil	Oil	6.1x10 ⁻² ± 0.1x10 ⁻²	0.5x10 ⁻³ ± 0.03x10 ⁻³

425 * HLB: Hydrophilic Lipophilic Balance

426

427
428
429
430
431
432
433

Table 2: Mean characterization of the different nanocarriers formulations

	Mean particle size (nm)	Polydispersity index (PI)	Zeta potential (mV)	Drug load (mg/g)	Encapsulation yield (%)
Blank LNC	50.3 ± 0.2	0.071 ± 0.003	-8.9 ± 1.2	-	-
Phtester LNC	53.4 ± 0.9	0.134 ± 0.005	-10.8 ± 2.0	2.5 ± 0.6	94 ± 3
Sucester LNC	57.8 ± 2.0	0.118 ± 0.009	-11.1 ± 1.3	3.1 ± 0.2	92 ± 6
Blank PCL-NC	289 ± 7.0	0.248 ± 0.011	-13.8 ± 0.5	-	-
Phtester PCL-NC	303 ± 12	0.323 ± 0.003	-18.2 ± 0.7	9.0 ± 1.1	72 ± 6
Sucester PCL-NC	295 ± 18	0.267 ± 0.006	-14.9 ± 2.4	7.3 ± 0.4	81 ± 2

434 Measurements were made in triplicates (n= 3) and results were expressed as mean values ± SD. Experimental drug load were
435 expressed as the amount of drug in milligrams per gram of lipid nanocapsules suspension. Encapsulation efficiency was
436 expressed as mean percentage (%) ± SD.

437
438
439
440

441

442 **Table 3:** Cytotoxicity (IC_{50}) of the indicated drugs on astrocytes, MDA-MB-231 and U87 cells.

443

$IC_{50}(\mu M)$ [95% CI]			
	Astrocytes	MDA-MB-231	U87
Blank PCL-NC	$7.4 \cdot 10^2$ [$1.4 \cdot 10^2$ - $9.6 \cdot 10^3$]	$1.8 \cdot 10^2$ [$0.6 \cdot 10^2$ - $2.7 \cdot 10^3$]	$4.0 \cdot 10^3$ [$2.6 \cdot 10^3$ - $1.2 \cdot 10^4$]
Blank LNC	$7.6 \cdot 10^2$ [1.9 - $2.2 \cdot 10^3$]	$3.0 \cdot 10^1$ [6.3 - $2.3 \cdot 10^2$]	$6.0 \cdot 10^3$ [$8.8 \cdot 10^1$ - $1.2 \cdot 10^4$]
PhtFerr	$3.7 \cdot 10^1$ [$1.3 \cdot 10^1$ - $3.3 \cdot 10^2$]	$2.0 \cdot 10^1$ [$1.3 \cdot 10^2$ - $2.3 \cdot 10^{-1}$]	$1.6 \cdot 10^{-1}$ [$3.8 \cdot 10^{-2}$ - $2.2 \cdot 10^{-1}$]
Phtester	$7.8 \cdot 10^2$ [1.0 - $7.1 \cdot 10^3$]	1.0 [0.28-5.6]	$9.2 \cdot 10^{-2}$ [$3.8 \cdot 10^{-2}$ - $2.2 \cdot 10^{-1}$]
Phtester-LNC	$8.0 \cdot 10^2$ [$2.1 \cdot 10^2$ - $2.1 \cdot 10^3$]	$2.1 \cdot 10^1$ [2.1 - $1.8 \cdot 10^2$]	$7.0 \cdot 10^{-2}$ [$2.1 \cdot 10^{-2}$ - $2.3 \cdot 10^{-1}$]
Phtester PCL-NC	$6.8 \cdot 10^2$ [$1.1 \cdot 10^2$ - $7.3 \cdot 10^2$]	$4.6 \cdot 10^1$ [5.1 - $2.4 \cdot 10^2$]	$7.6 \cdot 10^{-2}$ [$2.1 \cdot 10^{-2}$ - $2.3 \cdot 10^{-1}$]
SuccFerr	$3.4 \cdot 10^1$ [6.3 - $7.5 \cdot 10^1$]	$3.3 \cdot 10^{-1}$ [$4.7 \cdot 10^{-2}$ -1.0]	$2.7 \cdot 10^{-2}$ [$6.7 \cdot 10^{-3}$ - $1.1 \cdot 10^{-1}$]
Sucester	$7.1 \cdot 10^2$ [$2.1 \cdot 10^2$ - $1.0 \cdot 10^3$]	$6.0 \cdot 10^{-1}$ [$1.3 \cdot 10^{-1}$ - $9.4 \cdot 10^{-1}$]	$6.7 \cdot 10^{-2}$ [$1.3 \cdot 10^{-2}$ - $3.4 \cdot 10^{-2}$]
Sucester LNC	$7.0 \cdot 10^2$ [$1.2 \cdot 10^2$ - $8.1 \cdot 10^2$]	$1.8 \cdot 10^1$ [$1.5 \cdot 10^1$ - $1.4 \cdot 10^2$]	$4.6 \cdot 10^{-2}$ [$1.5 \cdot 10^{-2}$ - $1.4 \cdot 10^{-1}$]
Sucester-PCL-NC	$7.8 \cdot 10^2$ [$3.3 \cdot 10^2$ - $4.2 \cdot 10^3$]	$2.0 \cdot 10^1$ [$1.2 \cdot 10^1$ - $2.7 \cdot 10^1$]	$5.7 \cdot 10^{-2}$ [$1.2 \cdot 10^{-2}$ - $2.7 \cdot 10^{-1}$]
Tamoxifen	1.85 [0.94-3.62]	2,63 [0.39-17.94]	1.92 [0.57-6.38]

444

445

446 **References**

447

448 1. Jordan VC. Antiestrogens and selective estrogen receptor modulators as
449 multifunctional medicines. 1. Receptor interactions. *J Med Chem* 2003; 6: 883-908.

450 2. Fan P, Craig Jordan V. Acquired resistance to selective estrogen receptor modulators
451 (SERMs) in clinical practice (tamoxifen & raloxifene) by selection pressure in breast
452 cancer cell populations. *Steroids* 2014: 44-52.

453 3. Di Cristofori A *et al.* Continuous tamoxifen and dose-dense temozolomide in recurrent
454 glioblastoma. *Anticancer Res* 2013; 8: 3383-3389.

455 4. Jaouen G *et al.* The first organometallic selective estrogen receptor modulators
456 (SERMs) and their relevance to breast cancer. *Curr Med Chem* 2004; 18: 2505-2517.

457 5. Top S *et al.* Synthesis, Biochemical Properties and Molecular Modelling Studies of
458 Organometallic Specific Estrogen Receptor Modulators (SERMs), the Ferrocifens and
459 Hydroxyferrocifens: Evidence for an Antiproliferative Effect of Hydroxyferrocifens
460 on both Hormone-Dependent and Hormone-Independent Breast Cancer Cell Lines.
461 *Chemistry* 2003; 21: 5223-5236.

462 6. Jaouen G *et al.* Ferrocifen type anti cancer drugs. *Chem Soc Rev* 2015; 24: 8802-8817.

463 7. Richard MA *et al.* Oxidative metabolism of ferrocene analogues of tamoxifen:
464 characterization and antiproliferative activities of the metabolites. *Chem Med Chem*
465 2015; 6: 981-990.

466 8. Wang Y *et al.* Organometallic Antitumor Compounds: Ferrocifens as Precursors to
467 Quinone Methides. *Angew Chem Int Ed Engl* 2015; 35: 10230-10233.

- 468 9. Najlaoui F *et al.* Phthalimido-ferrocenylphenol cyclodextrin complexes:
469 Characterization and anticancer activity. *Int J Pharm* 2015; 1-2: 323-334.
- 470 10. Bruyere C *et al.* Ferrocifen derivatives that induce senescence in cancer cells: selected
471 examples. *Journal of Inorganic Biochemistry* 2014: 144-151.
- 472 11. Citta A *et al.* Evidence for targeting thioredoxin reductases with ferrocenyl quinone
473 methides. A possible molecular basis for the antiproliferative effect of
474 hydroxyferrocifens on cancer cells. *J Med Chem* 2014; 21: 8849-8859.
- 475 12. Wang Y *et al.* Ferrocenyl quinone methide-thiol adducts as new antiproliferative
476 agents: synthesis, metabolic formation from ferrocenophenols and oxidative
477 transformation. *Angew Chem Int Ed* 2016; 35.
- 478 13. Laine AL, Passirani C. Novel metal-based anticancer drugs: a new challenge in drug
479 delivery. *Curr Opin Pharmacol* 2012; 4: 420-426.
- 480 14. Huynh NT *et al.* Lipid nanocapsules: a new platform for nanomedicine. *Int J Pharm*
481 2009; 2: 201-209.
- 482 15. Allard E *et al.* Dose effect activity of ferrocifen-loaded lipid nanocapsules on a 9L-
483 glioma model. *Int J Pharm* 2009; 2: 317-323.
- 484 16. David S *et al.* Treatment efficacy of DNA lipid nanocapsules and DNA multimodular
485 systems after systemic administration in a human glioma model. *J Gene Med* 2012;
486 12: 769-775.
- 487 17. David S *et al.* siRNA LNCs--a novel platform of lipid nanocapsules for systemic
488 siRNA administration. *Eur J Pharm Biopharm* 2012; 2: 448-452.

- 489 18. Vanpouille-Box C *et al.* Tumor eradication in rat glioma and bypass of
490 immunosuppressive barriers using internal radiation with (188)Re-lipid nanocapsules.
491 *Biomaterials* 2011; 28: 6781-6790.
- 492 19. Vanpouille-Box C *et al.* Lipid nanocapsules loaded with rhenium-188 reduce tumor
493 progression in a rat hepatocellular carcinoma model. *PloS one* 2011; 3: e16926.
- 494 20. Griveau A *et al.* Silencing of miR-21 by locked nucleic acid-lipid nanocapsule
495 complexes sensitize human glioblastoma cells to radiation-induced cell death. *Int J*
496 *Pharm* 2013; 2: 765-774.
- 497 21. Letchford K, Burt H. A review of the formation and classification of amphiphilic
498 block copolymer nanoparticulate structures: micelles, nanospheres, nanocapsules and
499 polymersomes. *Eur J Pharm Biopharm* 2007; 3: 259-269.
- 500 22. Ali SAM *et al.* Mechanisms of polymer degradation in implantable devices. I.
501 Poly(caprolactone). *Biomaterials* 1993; 9: 648-656.
- 502 23. Yang X *et al.* In vitro and in vivo safety evaluation of biodegradable self-assembled
503 monomethyl poly (ethylene glycol)-poly (epsilon-caprolactone)-poly (trimethylene
504 carbonate) micelles. *J Pharm Sci* 2014; 1: 305-313.
- 505 24. Nga VD *et al.* Effects of polycaprolactone-based scaffolds on the blood-brain barrier
506 and cerebral inflammation. *Tissue Eng Part A* 2015; 3-4: 647-653.
- 507 25. Minick DJ *et al.* A comprehensive method for determining hydrophobicity constants
508 by reversed-phase high-performance liquid chromatography. *J Med Chem* 1988; 10:
509 1923-1933.

- 510 26. Heurtault B *et al.* A novel phase inversion-based process for the preparation of lipid
511 nanocarriers. *Pharm Res* 2002; 6: 875-880.
- 512 27. McCarthy KD, de Vellis J. Preparation of separate astroglial and oligodendroglial cell
513 cultures from rat cerebral tissue. *J Cell Biol* 1980; 3: 890-902.
- 514 28. Heurtault B *et al.* The influence of lipid nanocapsule composition on their size
515 distribution. *Eur J Pharm Sci* 2003; 1: 55-61.
- 516 29. Vonarbourg A *et al.* Evaluation of pegylated lipid nanocapsules versus complement
517 system activation and macrophage uptake. *J Biomed Mater Res A* 2006; 3: 620-628.
- 518 30. Vonarbourg A *et al.* Electrokinetic properties of noncharged lipid nanocapsules:
519 influence of the dipolar distribution at the interface. *Electrophoresis* 2005; 11: 2066-
520 2075.
- 521 31. Lamprecht A *et al.* New lipid nanocapsules exhibit sustained release properties for
522 amiodarone. *J Control Release* 2002; 1-2: 59-68.
- 523 32. Malzert-Freon A *et al.* Formulation of sustained release nanoparticles loaded with a
524 triptentone, a new anticancer agent. *Int J Pharm* 2006; 1-2: 157-164.
- 525 33. Peltier S *et al.* Enhanced oral paclitaxel bioavailability after administration of
526 paclitaxel-loaded lipid nanocapsules. *Pharm Res* 2006; 6: 1243-1250.
- 527 34. Li Y *et al.* Mechanisms of U87 astrocytoma cell uptake and trafficking of monomeric
528 versus protofibril Alzheimer's disease amyloid-beta proteins. *PloS one* 2014; 6:
529 e99939.

530 35. Xu R *et al.* An injectable nanoparticle generator enhances delivery of cancer
531 therapeutics. *Nat Biotechnol* 2016; 4: 414-418.

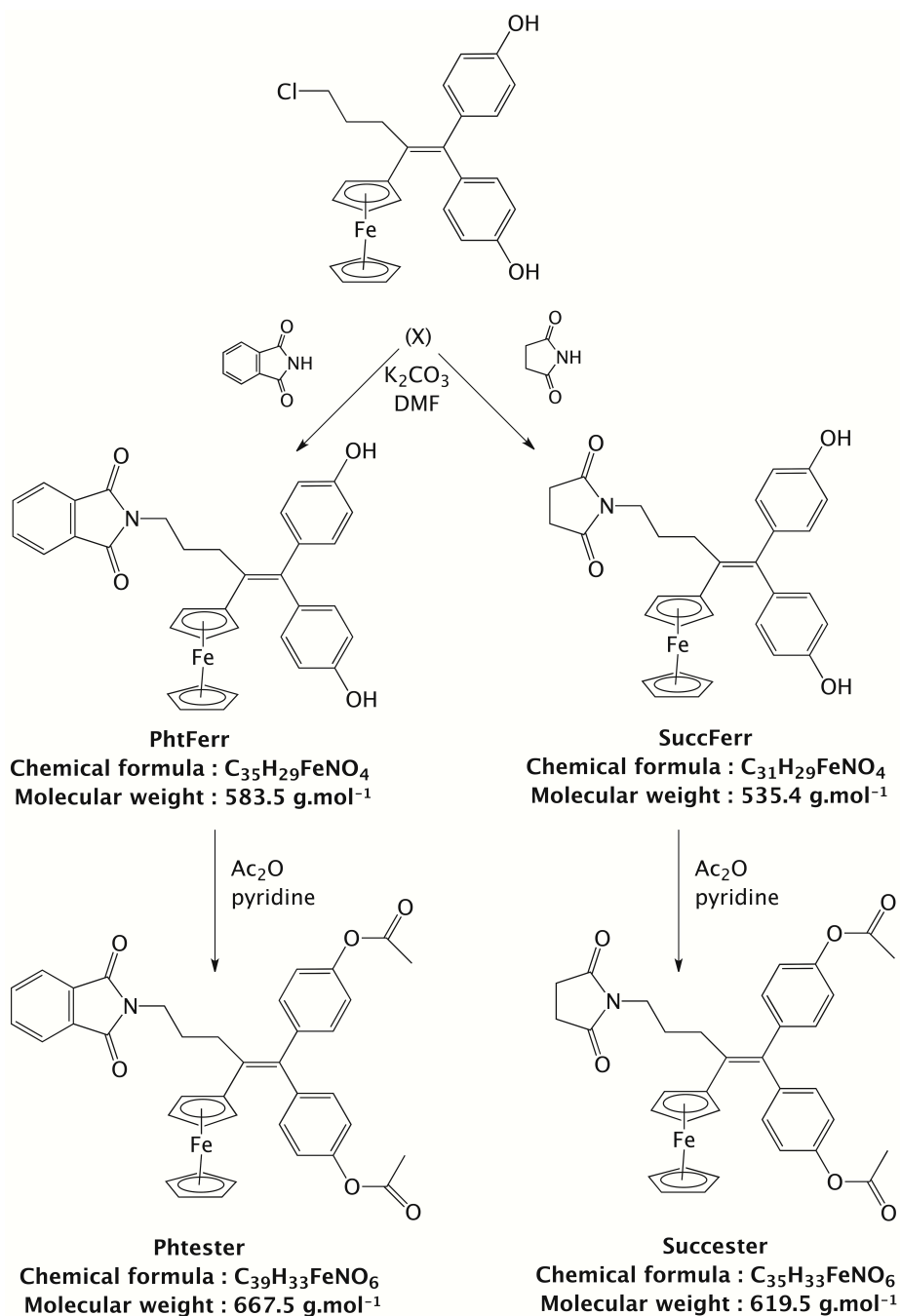
532 36. Aparicio-Blanco J, Torres-Suárez A-I. Glioblastoma Multiforme and Lipid
533 Nanocapsules: A Review. *J Biomed Nanotechnol* 2015; 8: 1283-1311.

534

535

536 **Figure 1.** Chemical structure and synthesis of the main compounds: Phthalimido-ester (**Phtester**) and
537 Succinimido-ester (**Succester**) by acetylation of **PhtFerr** and **SuccFerr**. Synthesis of these precursors
538 by substitution reaction on the chlorinated alkene **X** using phthalimide or succinimide.

539



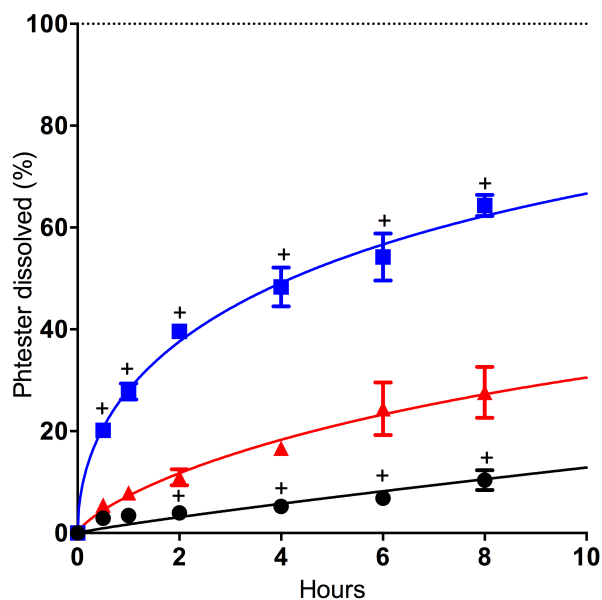
540

541

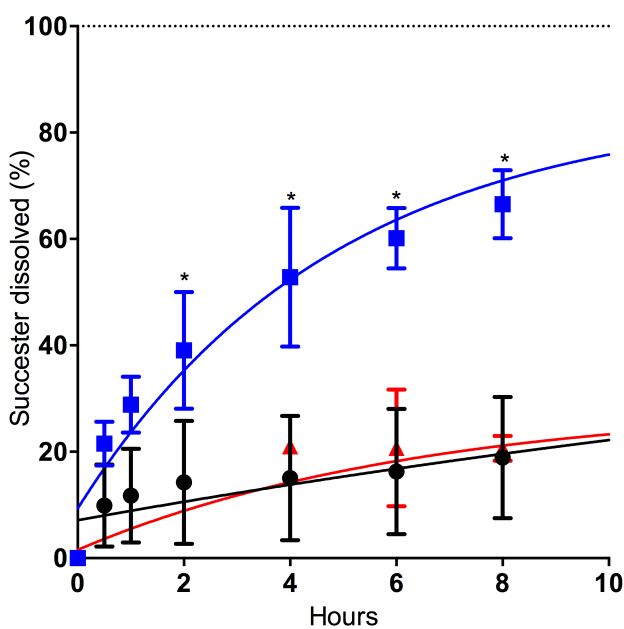
542

543 **Figure 2.** Release profiles of a) Phtester [from Phtester (-▲-), Phtester LNC (-●-), Phtester PCL-NC
 544 (-■-)] and b) Succester [from Succester (-▲-), Succester LNC (-●-), and Succester PCL-NC (-■-)] by
 545 dialysis in Tween[®] 20 (1%) ; + different vs Phtester, p < 0.05 (Mann and Whitney) ; * different vs
 546 Succester, p < 0.05 (Mann and Whitney).

547



548



549

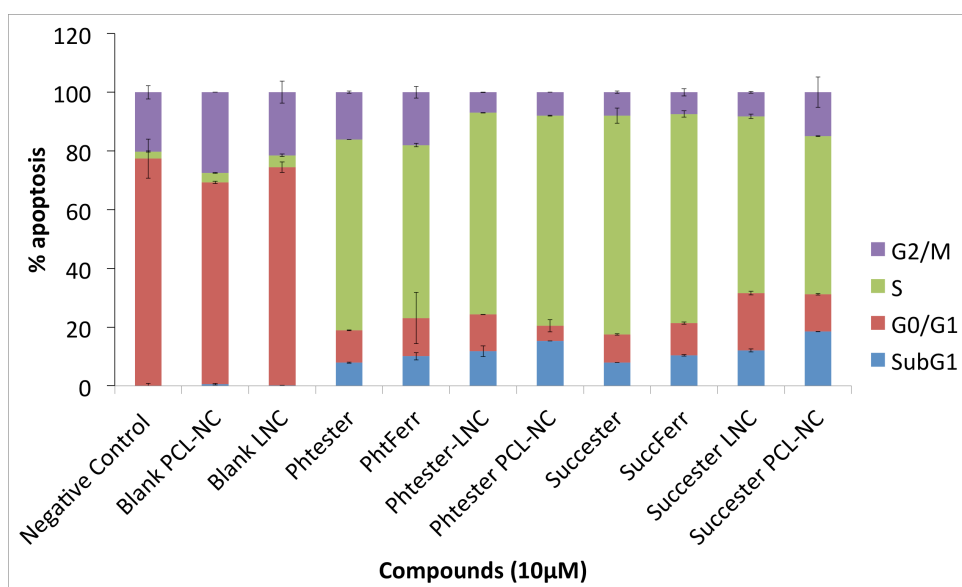
550

551

552

Figure 3. Cell cycle distribution

553



554

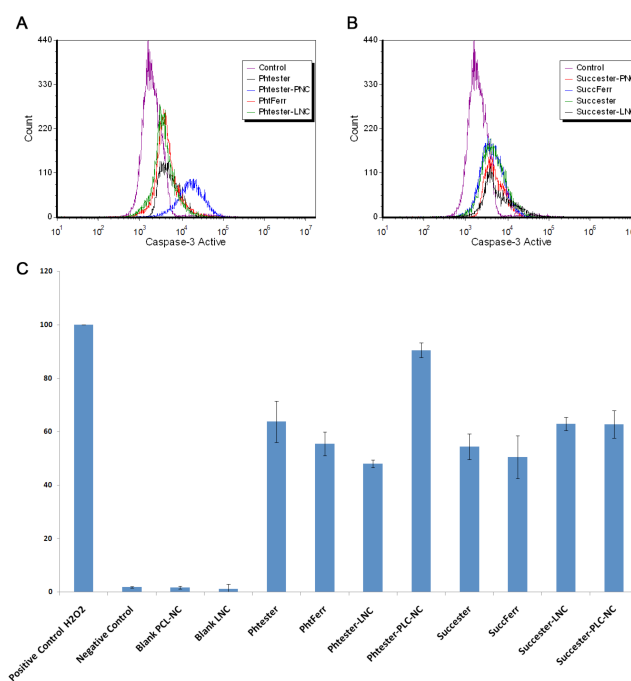
555

Figure 4. Apoptosis counting (panel a-b) and percentage of caspase-3 active cells (panel c) after 96 h of treatment

556

557

558



559

560 **Supplementary Materials for the Chemistry Section:**

561 **Chemical Reagents**

562

563 The starting materials for the synthesis were acetic anhydride, pyridine, hydrochloric acid,
564 sodium hydroxide, tetrahydrofuran (THF) magnesium sulfate, cyclohexane and ethyl acetate
565 which were obtained from Sigma–Aldrich (L’Isle d’Abeau Chesnes, 38297 Saint-Quentin,
566 Fallavier, France), TCI EUROPE N.V. (Boerenveldseweg 6, Haven 1063, 2070 Zwijndrecht,
567 Belgique), and Alfa Aesar France (2 allée d’Oslo, 67300 Schiltigheim, France).

568 All reactions and manipulations were carried out under an argon atmosphere using standard
569 Schlenk techniques. THF was distilled over sodium/benzophenone prior to use. Thin layer
570 chromatography was performed on silica gel 60 GF₂₅₄. IR spectra were obtained on a FT/IR-
571 4100 JASCO 180 spectrometer. ¹H and ¹³C NMR spectra were acquired on a Bruker 300
572 MHz spectrometer. Mass spectrometry was carried out at the “Service de Spectrométrie de
573 Masse” at ENSCP, Paris. High-resolution mass spectra (HRMS) were acquired in the “Institut
574 Parisien de Chimie Moléculaire (IPCM – UMR 8232)” at the “Université Pierre et Marie
575 Curie”, Paris. Microanalyses were performed by the “Service de Microanalyse ICSN” at Gif
576 sur Yvette, France. We already described the synthesis of **PhtFerr** compounds elsewhere (7).
577 Measurements of the octanol/water partition coefficient (log Po/w) were made by the HPLC
578 technique according to a method described previously (see ref 21). Measurement of the
579 chromatographic capacity factors (k) for each molecule was done at various concentrations in
580 the range of 95–75% methanol containing 0.25% (v/v) 1-octanol and an aqueous phase
581 consisting of 0.15% (v/v) n-decylamine in the buffering agent MOPS (3-morpholinopropane-
582 1-sulfonic acid, prepared in 1-octanol saturated water) adjusted to pH 7.4. These capacity
583 factors (k’) are extrapolated to 100% of the aqueous component given the value of k’_w. The
584 log Po/w is obtained by the formula $\log Po/w = 0.13418 + 0.98452 \log k'$.

585

586 The lipophilic Labrafac® CC (caprylic/capric acid triglycerides) was provided by Gattefosse
587 S.A. (Saint-Priest, France). Lipoïd® S75-3 (soybean lecithin at 69% of phosphatidylcholine)
588 was a gift from Lipoïd GmbH (Ludwigshafen, Germany); Solutol® HS15 (a mixture of free
589 polyethylene glycol 660 and polyethylene glycol 660 hydroxystearate) was from Sigma-
590 Aldrich (Saint Quentin Fallavier, France). Other reactants were obtained from Prolabo

591 (Fontenay-sous-bois, France). Deionised water was obtained from a Milli-Q plus system
592 (Millipore, Paris, France).

593 Poly(ϵ -caprolactone) (PCL), triethylcitrate and Pluronic (F 68 or F 127) were purchased from
594 Sigma-Aldrich (Saint-Quentin Fallavier, France). Egg lecithin was obtained from VWR
595 (Fontenais-sous-Bois, France), Dulbecco modified Eagle medium (DMEM) with glucose and
596 l-glutamine (Cergy-Pontoise, France), foetal calf serum (FCS) (BioWhittaker) and antibiotic
597 and antimycotic solution (Sigma, Saint-Quentin Fallavier, France).

598

599 **Synthesis of SuccFerr :**

600 ***N*-{4-ferrocenyl-5,5-bis-(4-hydroxyphenyl)-pent-4-enyl}succinimide (SuccFerr):**

601 A mixture of potassium carbonate (0.478 g, 3.5 mmoles) and succinimide (0.457 g, 4.6
602 mmoles) in dimethylformamide (DMF) was heated at 80°C for 15 min. The compound **X** (5-
603 chloro-2-ferrocenyl-1,1-bis-(4-hydroxyphenyl)-pent-1-ene, 1.09 g, 2.31 mmoles) was added
604 and the stirring was continued at 80°C overnight. The mixture was allowed to cool to room
605 temperature, was poured into a diluted hydrochloric acid solution, was extracted twice with
606 diethyl ether, then the organic layer was dried on magnesium sulfate and concentrated under
607 reduced pressure. The residue was purified by flash-chromatography (ethyl acetate) to afford
608 the imide **SuccFerr** that was obtained as an orange solid with a yield of 54% (0.662 g). mp:
609 225°C decomp. The corresponding NMR profile is described hereafter in the mass
610 spectrometry section.

611

612 **Synthesis of Phtester:**

613 ***N*-{4-ferrocenyl-5,5-bis-(4-acetoxyphenyl)-pent-4-enyl}phthalimide (Phtester):**

614 Acetic anhydride (10 mL) was added dropwise to a solution of PhtFerr (3.01 g, 5.16 mmol)
615 and pyridine (1.63 g, 1.7 mL, 20.6 mmol) in dry THF (50 mL) at RT then the reaction mixture
616 was stirred at RT overnight. The solution was then poured into water (300 mL) in presence of
617 hydrochloric acid (10 mL) and dichloromethane (300 mL) and the layers were separated. The
618 aqueous layer was extracted twice with dichloromethane and the combined organic layers
619 were washed with a solution of sodium hydroxide (2 g in 300 mL of water), then with water.
620 The solution was dried over magnesium sulfate and concentrated under reduced pressure.

621 Flash chromatography (cyclohexane/ethyl acetate 1/1) then recrystallization from ethyl
622 acetate yielded the pure product as an orange solid (2.87 g, 84 %). Mp: 210°C. The
623 corresponding NMR profile is described hereafter in the mass spectrometry section. The
624 partition coefficient of the obtained **Phtester** was the following: Log Po/w: 6.09. This
625 corresponds to a high hydrophobicity profile.

626

627 **Synthesis of Succester:**

628 ***N*-{4-ferrocenyl-5,5-bis-(4-acetoxyphenyl)-pent-4-enyl}succinimide (Succester):**

629 Acetic anhydride (18 mL) was added dropwise to a solution of SuccFerr (5 g, 9.34 mmol) and
630 pyridine (2.95 g, 3.1 mL, 37.3 mmol) in dry THF (80 mL) at RT then the reaction mixture
631 was stirred at RT overnight. The solution was then poured into water (400 mL) in addition to
632 hydrochloric acid (15 mL) and dichloromethane (400 mL) and the layers were separated. The
633 aqueous layer was extracted twice with dichloromethane and the combined organic layers
634 were washed with a solution of sodium hydroxide (3 g in 400 mL of water), then with water.
635 The solution was dried over magnesium sulfate and concentrated under reduced pressure.
636 Flash chromatography (cyclohexane/ethyl acetate 1/1) then recrystallization from ethyl
637 acetate yielded the pure product as an orange solid (5.3 g, 92 %). Mp: 157°C. The
638 corresponding NMR profile is described hereafter in the mass spectrometry section. The
639 partition coefficient of the obtained **Succester** was the following: Log Po/w: 5.18. This
640 corresponds to a high hydrophobicity profile.

641

642 **Mass spectrometry: characterization of the products**

643 ***N*-{4-ferrocenyl-5,5-bis-(4-hydroxyphenyl)-pent-4-enyl}succinimide (SuccFerr):**

644 ¹H NMR (300 MHz, acetone-d₆) : δ 1.70-1.81 (m, 2H, CH₂), 2.56-2.64 (m, 6H, 2CH₂
645 succ+CH₂-C=C), 3.38 (t, *J* = 6.6 Hz, 2H, CH₂N), 3.95 (t, *J* = 1.9 Hz, 2H, C₅H₄), 4.10 (t, *J* =
646 1.9 Hz, 2H, C₅H₄), 4.16 (s, 5H, Cp), 6.74 (d, *J* = 8.6 Hz, 2H, C₆H₄), 6.85 (d, *J* = 8.6 Hz, 2H,
647 C₆H₄), 6.91 (d, *J* = 8.6 Hz, 2H, C₆H₄), 7.04 (d, *J* = 8.6 Hz, 2H, C₆H₄), 8.25 (s, 1H, OH), 8.36
648 (s, 1H, OH). ¹³C NMR (75 MHz, acetone-d₆) : δ 29.4 (2CH₂, succinimide), 30.8 (CH₂), 33.8
649 (CH₂), 39.7 (CH₂), 69.5 (2CH, C₅H₄), 70.7 (5CH, Cp+2CH, C₅H₄), 88.8 (C, C₅H₄), 116.5
650 (2CH, C₆H₄), 116.6 (2CH, C₆H₄), 132.0 (2CH, C₆H₄), 132.4 (2CH, C₆H₄), 135.3 (C), 137.7

651 (C), 137.9 (C), 140.2 (C), 157.3 (C), 157.5 (C), 178.6 (2CO). IR (KBr, ν cm^{-1}): 3421 (OH),
652 3096, 2967, 2936 (CH, CH_2), 1697 (CO). MS (ESI) m/z : 535 $[\text{M}]^+$, 342, 279, 224, 143, 83.
653 HRMS (ESI, $\text{C}_{31}\text{H}_{29}\text{FeNO}_4$: $[\text{M}]^+$) calcd: 535.1446, found: 535.1460. Anal. Calcd for
654 $\text{C}_{31}\text{H}_{29}\text{FeNO}_4(\text{H}_2\text{O})_{0.3}$: C, 68.85; H, 5.51; N, 2.58. Found: C, 68.76; H, 5.14; N, 2.37.

655 ***N*-{4-ferrocenyl-5,5-bis-(4-acetoxyphenyl)-pent-4-enyl}phthalimide (Phtester):**

656 ^1H NMR (DMSO- d_6): δ 1.70-1.89 (m, 2H, CH_2), 2.24 (s, 6H, Me), 2.42-2.49 (m, 2H, CH_2),
657 3.50 (t, $J = 6.4$ Hz, 2H, CH_2N), 3.79 (t, $J = 1.7$ Hz, 2H, C_5H_4), 4.10 (s, 7H, Cp + C_5H_4), 6.89
658 (d, $J = 8.5$ Hz, 2H, C_6H_4), 7.02 (d, $J = 8.8$ Hz, 2H, C_6H_4), 7.06 (d, $J = 8.8$ Hz, 2H, C_6H_4), 7.16
659 (d, $J = 8.5$ Hz, 2H, C_6H_4), 7.86 (s, 4H, phthalimide). ^{13}C NMR (DMSO- d_6): δ 20.8 (2 CH_3),
660 29.3 (CH_2), 31.5 (CH_2), 37.3 (CH_2), 68.2 (2CH, C_5H_4), 68.7 (2CH, C_5H_4), 69.1 (5CH, Cp),
661 85.3 (C, C_5H_4), 121.4 (2CH, C_6H_4), 121.7 (2CH, C_6H_4), 122.9 (2CH, phthalimide), 129.5
662 (2CH, C_6H_4), 130.1 (2CH, C_6H_4), 131.4 (2C, phthalimide), 134.3 (2CH, phthalimide), 135.4
663 (C), 136.2 (C), 140.9 (C), 141.4 (C), 148.7 (C), 148.9 (C), 167.8 (2CO, phthalimide), 168.8
664 (COO), 169.0 (COO). IR (KBr, ν cm^{-1}): 3454 (OH), 1766, 1752, 1708 (CO). HRMS (ESI,
665 $\text{C}_{39}\text{H}_{33}\text{FeNNaO}_6$: $[\text{M}+\text{Na}]^+$) calcd: 690.154948, found: 690.15422.

666 ***N*-{4-ferrocenyl-5,5-bis-(4-acetoxyphenyl)-pent-4-enyl}succinimide (Succester):**

667 ^1H NMR (acetone- d_6): δ 1.68-1.85 (m, 2H, CH_2), 2.23 (s, 3H, CH_3), 2.27 (s, 3H, CH_3), 2.50-
668 2.66 (m, 6H, 2 CH_2 succinimide + $\text{CH}_2\text{-C}=\text{C}$), 3.37 (t, $J = 6.5$ Hz, 2H, CH_2N), 3.91 (s, 2H,
669 C_5H_4), 4.11 (s, 2H, C_5H_4), 4.15 (s, 5H, Cp), 7.01 (d, $J = 8.2$ Hz, 2H, C_6H_4), 7.11 (d, $J = 8.2$
670 Hz, 2H, C_6H_4), 7.12 (d, $J = 8.2$ Hz, 2H, C_6H_4), 7.26 (d, $J = 8.2$ Hz, 2H, C_6H_4). ^{13}C NMR
671 (acetone- d_6): δ 21.00 (CH_3), 21.03 (CH_3), 28.7 (2 CH_2 , succinimide), 29.8 (CH_2), 33.1 (CH_2),
672 38.9 (CH_2), 69.2 (2CH, C_5H_4), 70.1 (5CH, Cp + 2CH, C_5H_4), 86.9 (C, C_5H_4), 122.5 (2CH,
673 C_6H_4), 122.6 (2CH, C_6H_4), 131.0 (2CH, C_6H_4), 131.4 (2CH, C_6H_4), 137.1 (C), 137.7 (C),
674 142.5 (C), 142.8 (C), 150.4 (C), 150.5 (C), 169.5 (COO), 169.7 (COO), 177.9 (2CO). IR
675 (KBr, ν cm^{-1}): 3443 (OH), 1764, 1752, 1697 (CO). HRMS (ESI, $\text{C}_{35}\text{H}_{33}\text{FeNNaO}_6$: $[\text{M}+\text{Na}]^+$)
676 calcd: 642.154948, found: 642.15387. Anal. Calcd for $\text{C}_{35}\text{H}_{33}\text{FeNO}_6(\text{H}_2\text{O})_{0.5}$: C, 66.88; H,
677 5.44; N, 2.23. Found: C, 67.26; H, 5.36; N, 2.09.

678

679